Shear Breakage of Nylon Membrane Microcapsules in a Turbine Reactor

Denis Poncelet and Ronald J. Neufeld
Department of Chemical Engineering, McGill University, 3480 University Street, Montreal, H3A 2A7 Canada

Accepted for publication December 18, 1987

The breakage of nylon membrane microcapsules is proposed as a new method to study and quantify shear effects in biological systems. A critique of this method shows that a narrower particle size distribution may be an important improvement in the breakage study as well as breakage control in many bioreactor and biotechnological applications. In a turbine reactor, it was shown that the primary process which determines the microcapsule breakage is the shear effect. The breakage kinetics are first order with regard to the microcapsule concentration. The breakage kinetic constant was observed to be dependent on the temperature and the particle size, and proportional to the average shear rate and the third power of the turbine angular velocity. Decrease of the breakage kinetic constant with temperature can be explained by a decrease of fluid viscosity and a change in nylon membrane properties. An increase in the breakage kinetic constant with the microcapsule diameter can be due to a lowering of internal pressure and a reduction of the membrane resistance with size. Proportionality between the breakage kinetic constant and the shear rate shows that shear is the main process which leads to microcapsule breakage. The additional intervention in the shear rate expression of the turbine angular speed in the form of the turbine and particle velocities, results in the dependence of the breakage kinetic constant on the third power of the angular velocity.

INTRODUCTION

Fluids which are animated by mixing or flow are subjected to velocity gradients. These gradients induce shear stresses which lead to medium homogenization. However, if particles are suspended in the fluid, a deformation or breakage of the particles may result. Pumping and mixing, both associated with flow, may cause enzyme molecular distortion or stretching, leading to reduction of reaction rate or breakage of molecular bonds resulting in enzyme inactivation.[1-3] In biological reactors, shear fields lead to bacterial cell disruptions,[4,5] decrease of growth rate,[5] reduction of filamentous cell length,[5] and change in cell morphology.[4,6] In the fluidized bed, the biological aggregate size and form are determined in large part by shear effects.[7]

Shear effects are often ignored in control and optimization of biological processes while mixing and environmental effects are frequently considered. Due to the complexity of the shear problem, only a few studies have lead to a quantitative relationship between determinant parameters of shear and the effect on particle breakage. Urease microcapsules have been observed to rupture in CSTR studies,[8] resulting in release of enzyme. In biomedical applications, this presents significant problems when foreign protein (enzyme) is released to blood plasma. The ultrathin membrane, surrounding intact microcapsules, provides a semipermeable barrier between the biocatalyst and plasma components.

A study on the disruption of microcapsules in a turbine reactor may serve as a useful starting point to examine the effects of shear on a variety of biological systems. The physical structure of the microcapsule is well defined and controlled, and the membrane skin surrounding the spherical capsule may simulate the membrane around biological cells. Damage to a microcapsule membrane results in release of contents which are well defined and quantifiable, while damage to a mammalian, plant, or microbial cell may be more difficult to define given the irregular shape of the cell and the complex and variable nature of the contents and internal structure.

MATERIALS AND METHODS

Microcapsule Preparation

Dextran, with an average molecular weight of 1.72×10^4 (Sigma, D-4626) was encapsulated within a nylon membrane following the procedure for enzyme encapsulation described by Chang.[9] An aqueous dextran solution [10% (w/v)] containing one of the nylon monomers (1,6-Hexadiamine, Kodac, 5932) is dispersed with help of an emulsifier (Span 85, Atkemix Inc.) in an organic phase [1/4 (v/v) Cloroform, A&C, C-270, and Cyclohexane, A&C, C-463]. The second monomer, soluble in the organic phase (Terephtaloyl chloride, Aldrich, 12 087-1), is introduced to the emulsion. The nylon polymerization process takes place at the aqueous droplet interface. Microcapsules are washed with a 50% followed by a 1% solution of Tween 20 (Aldrich, 12087-1).

Biotechnology and Bioengineering, Vol. 33, Pp. 95–103 (1989)

CCC 0006-3592/89/010095–09$04.00

Microcapsule sample preparations were sieved for size separation under water with gentle mixing so as to reduce the packing and breakage of the microcapsules on the screen.

Turbine Reactor

The apparatus used for the shear experiments consisted of a standard[10] flat-bottom cylindrical plexiglass tank with four baffles, stirred by a six-blade turbine. Reactor and turbine configuration are illustrated in Figure 1.

Experimental Procedure

A suspension containing 10% (v/v) microcapsules in water was agitated in the reactor under a range of mixing speeds (200–500 rpm). Aliquots were filtered (0.45-μm membrane filter) and dextran concentration of the supernatant determined by the sulfuric–phenol method.[11]

The concentration of dextran following total disruption of microcapsules was determined as described above after breakage of the microcapsule suspension by agitation with 1-mm-diameter glass beads by means of a magnetic stir bar for 0.5 h. Complete disruption of microcapsules was observed microscopically.

Microcapsule diameters were determined microscopically using a graduated monocle. Size distribution was obtained by measuring 400 diameters (Fig. 2). Mean diameter, $\langle d \rangle$, and mean volume, $\langle v \rangle$, were computed using eqs. (1) and (2):

$$\langle d \rangle = \frac{\sum_i n_i d_i}{\sum_i n_i} \tag{1}$$

$$\langle v \rangle = 6\pi \frac{\sum_i n_i d_i^3}{\sum_i n_i} \tag{2}$$

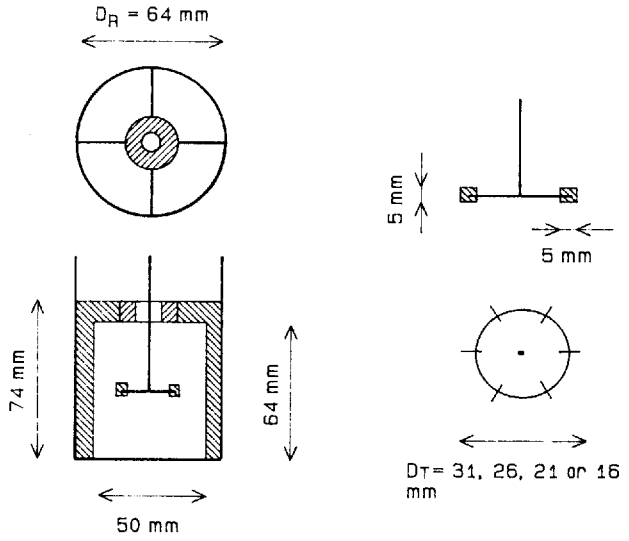

Figure 1. Reactor and turbine geometry.

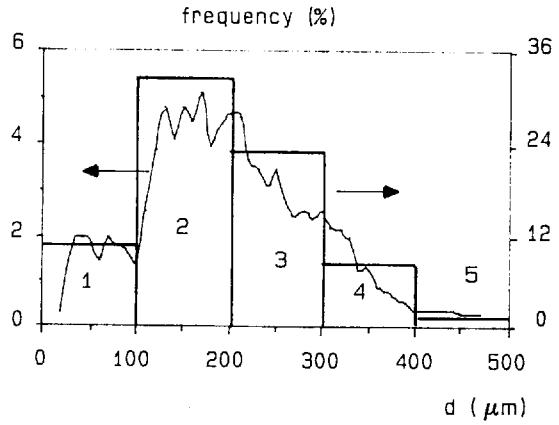

Figure 2. Microcapsule size distribution and size class partition: $(\langle d \rangle_0 = 200\ \mu m$; $\sigma_d = 90\ \mu m$; $D_R = 31$ mm; $\omega = 31.4\ s^{-1}$; and $T \approx 20°C)$.

where n_i is the number of microcapsules having a diameter d_i.

RESULTS

Data Acquisition

The volumetric fraction of nonbroken microcapsules, F_v, at any time t, can be determined from the dextran concentration using eq. (3).

$$F_v(t) = \frac{V_t}{V_0} = \frac{[\text{dextran}]_\infty - [\text{dextran}]_t}{[\text{dextran}]_\infty - [\text{dextran}]_0} \tag{3}$$

where V is the total volume of nonbroken microcapsules, subscript 0 refers to $t = 0$, and subscript ∞ to $t = \infty$, when all microcapsules are broken. Figure 3 illustrates the evolution with time of the nonbroken volumetric fraction, F_v, representing significant breakage of the microcapsules following a 90-min experimental period.

The mean microcapsule volume, $\langle v \rangle$, decreased with time, t, as shown in Figure 4. The total volume of nonbroken microcapsules, V, at a given time, t, is given by the product of the number, N, and the mean volume, $\langle v \rangle$:

$$V_t = N_t \langle v \rangle_t \tag{4}$$

Dividing eq. (4) for time t by eq. (4) for time 0, and combining with eq. (3), leads to an expression for the numeric fraction of the nonbroken microcapsules, F_n:

$$F_n = \frac{N_t}{N_0} = \frac{V_t/\langle v \rangle_t}{V_0/\langle v \rangle_0} = F_v \frac{\langle v \rangle_0}{\langle v \rangle_t} \tag{5}$$

Figure 5 shows the evolution of the nonbroken numeric fraction, F_n, with time, t. Assuming a given evolution of the numeric fraction, F_n, eq. (7) permits a computation of the change in volumetric fraction, F_v, for different levels of decrease in the mean volume, $\langle v \rangle$, (Fig. 6). This simulation was performed assuming an exponential decrease of the mean microcapsule volume, $\langle v \rangle$ (according to Fig. 4).

The evolution of the mean microcapsule volume, $\langle v \rangle$, with time, t, during the experiment reflects a breakage rate

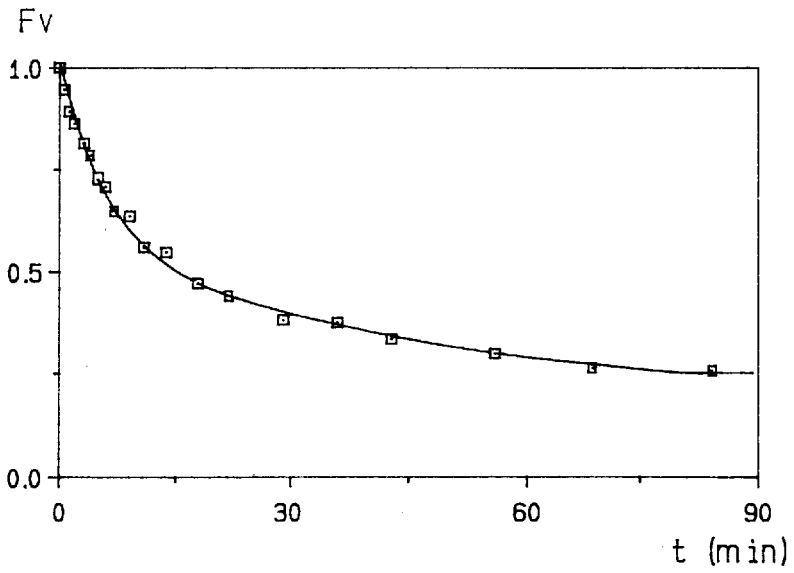

Figure 3. Evolution with time of the nonbroken volumetric fraction, F_v ($\langle d \rangle_0$ = 200 μm; σ_d = 90 μm; D_R = 31 mm; ω = 31.4 s^{-1}; and $T \approx 20$°C).

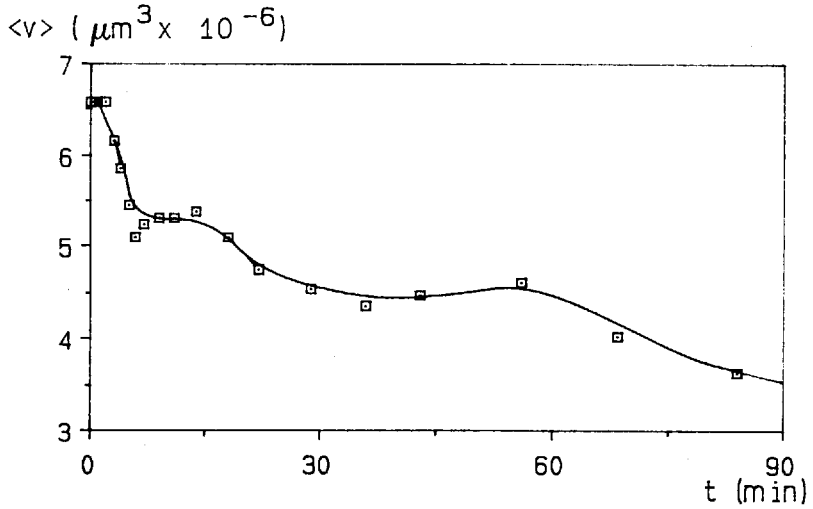

Figure 4. Mean microcapsule volume, $\langle v \rangle$, evolution with time ($\langle d \rangle_0$ = 200 μm; σ_d = 90 μm; $\langle d \rangle_{84\ min}$ = 168 μm; σ_d = 66 μm; D_R = 31 mm; ω = 31.4 s^{-1}; and $T \approx 20$°C).

dependent on the microcapsule size. It leads to an evolution with time of the sample breakage characteristics. To resolve this problem, a sieving was simulated by software. The microcapsules were divided into several size classes (Fig. 2). At a given time, t, the number of nonbroken microcapsules in a class c, $N_t(c)$, is given by:

$$N_t(c) = N_t \varphi(t, c) \tag{6}$$

where $\varphi(t, c)$ gives the fraction of microcapsules at time t and in size class c. Recalling eq. (5) and dividing eq. (6) by itself for time t and 0 leads to:

$$F_n(t, c) = \frac{N_t(c)}{N_0(c)} = \frac{N_t \varphi(t, c)}{N_0 \varphi(0, c)} = F_n(t) \frac{\varphi(t, c)}{\varphi(0, c)} \tag{7}$$

where $F_n(t, c)$ is the nonbroken numeric fraction for size class c. The evolution with time of the nonbroken numeric fraction for the different size classes during one experiment is presented in Figure 7. The mean volume of a given size class remained relatively constant during the experiment.

The nonbroken numeric fraction for a given size class, $F_n(c)$, was obtained from seven experimental values: dextran concentration at time 0, t, and ∞, mean volume, $\langle v \rangle$, at time 0 and t, and size class fraction, φ, at time 0 and t. Even if the data acquisition errors remain small, it leads to a large noise in the non-broken numeric fraction, $F_n(c)$, for a given size class. This problem was partially resolved by a smoothing of the raw data as done in Figure 7.

Breakage Kinetic Analysis

The evolution with time of the nonbroken numeric fraction, F_n, may be linearized for a given order with regard to the microcapsule concentration as illustrated in Figure 8:

$$\text{Zero order:} \qquad F_n = 1 - k_0 t \tag{8}$$

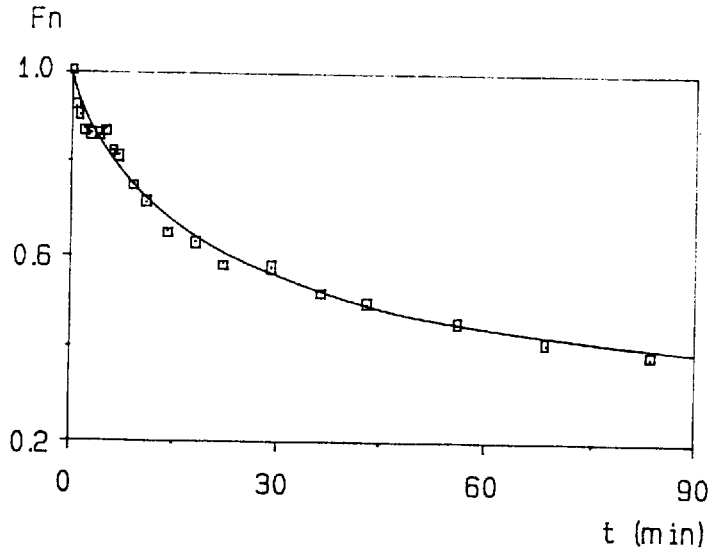

Figure 5. Nonbroken numeric fraction, F_n, evolution with time, t: ($\langle d \rangle_0$ = 200 μm; σ_d = 90 μm; D_R = 31 mm; ω = 31.4 s^{-1}; and $T \approx 20$°C).

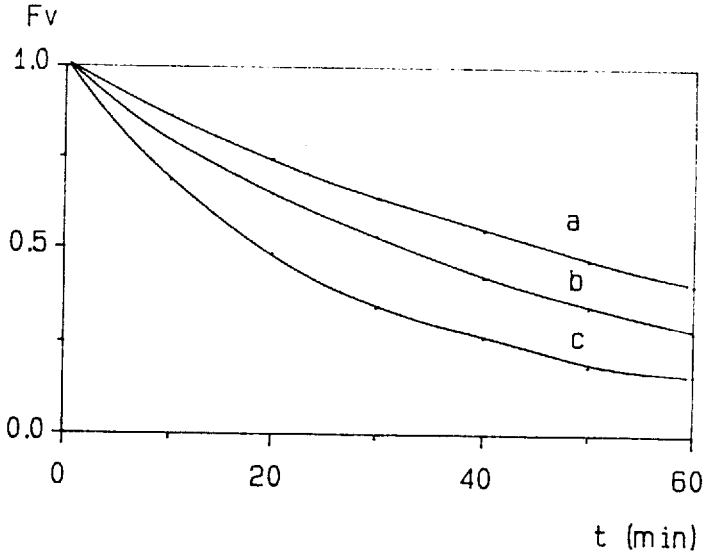

Figure 6. Effect of the mean microcapsule volume, $\langle v \rangle$, on the nonbroken volumetric fraction, F_v: (a) $\langle v \rangle$ = 100%; (b) $\langle v \rangle$ = 90%; and (c) $\langle v \rangle$ = 75% of the initial mean microcapsule volume, $\langle v \rangle_0$, at time t = 60 min.

First order: $$\ln F_n = -k_1 t \quad (9)$$

Second order: $$1/F_n = 1 + k_2 t \quad (10)$$

The zero order may be rejected because the plotting of smoothed data following eq. (8) is non-linear (Fig. 8).

For the true reaction order, the kinetic constant is a true constant and doesn't depend on the initial microcapsule concentration. Table I presents the values of the breakage kinetic constant for the first and the second order, k_1 and k_2, and for two different initial microcapsule concentrations. The breakage kinetic constant for the second order, k_2, varied with the initial microcapsule concentration, while the first-order constant, k_1, remained relatively constant. On this basis, it was assumed to be first order kinetics for the microcapsule breakage.

The influence of four parameters, temperature, T, microcapsule size, d, turbine diameter, D_T, and turbine angular velocity, ω, on the breakage kinetic constant, k_1, was studied. Table II illustrates the strong dependence of the breakage kinetic constant, k_1, on temperature, T. The fluid viscosity, η, at the two temperatures under consideration is also presented in Table II. A linear relation between the breakage kinetic constant, k_1, and the fourth power of the microcapsule diameter, d, was observed in Figure 9.

The flow conditions around a turbine blade are largely unknown.[12] In a turbine reactor, the shear rate is not uniform and different parameters may be used to define it. As a first and simple approximation, the linear average shear rate, $\langle \gamma \rangle$, can be computed by:

$$\langle \gamma \rangle = 2\omega D_T/(D_R - D_T) \quad (11)$$

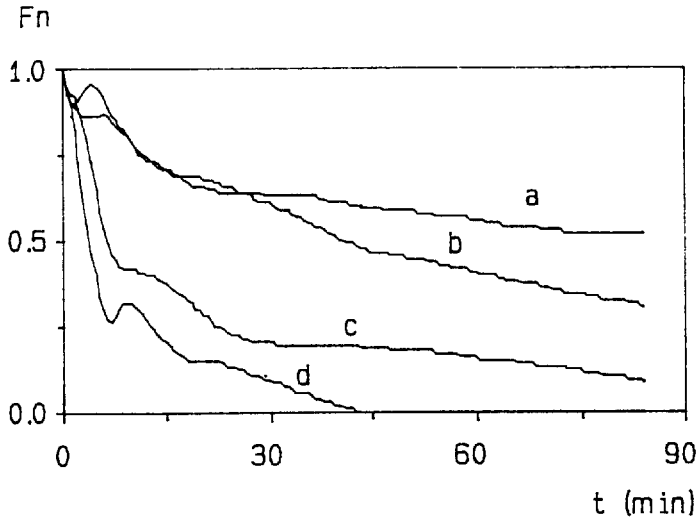

Figure 7. Nonbroken numeric fraction in a given class, $F_n(c)$, with time, t (a) $\langle d \rangle_0 = 150$ μm; (b) $\langle d \rangle_0 = 250$ μm; (c) $\langle d \rangle_0 = 350$ μm; and (d) $\langle d \rangle_0 = 450$ μm ($D_R = 31$ mm; $\omega = 31.4$ s^{-1}; and $T \approx 20$°C).

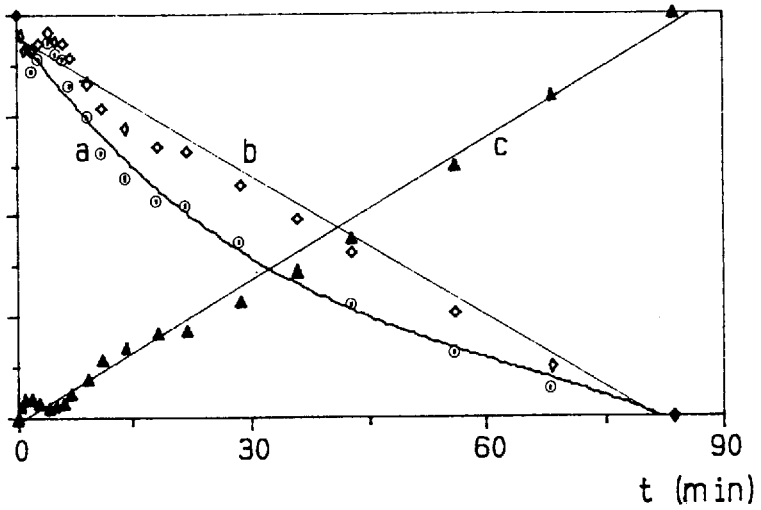

Figure 8. Time evolution of the nonbroken numeric fraction, F_n according to: (a) eq. (8) (zero order), (b) eq. (9) (first order), (c) eq. (10) (second order) ($\langle d \rangle_0 = 250$ μm; $\sigma_d = 30$ μm; $D_R = 31$ mm; $\omega = 31.4$ s^{-1}; and $T \approx 20$°C).

where ω is the turbine angular velocity; D_T is the turbine diameter; and D_R is the reactor diameter. The turbine, in this approximation, is likened to a cylinder of the same diameter and the hydrodynamic regime is assumed to be laminar. At constant turbine angular velocity, ω, the breakage kinetic constant, k_1, was found linearly correlated with the geometric terms of eq. (11) (Fig. 10). The breakage kinetic constant, k_1, was also seen to be proportional to the third power of the turbine angular velocity, ω (Fig. 11).

Table I. Effect of the initial microcapsule concentration on the breakage kinetic constants, k_1 and k_2.

Initial microcapsule concentration [% (v/v)]	k_1 (s^{-1})	k_2 (s^{-1})
8	8.0×10^{-2}	8.5×10^{-3}
21	6.7×10^{-2}	2.4×10^{-3}

Note: $\langle d \rangle_0 = 400$ μm; $\sigma_d = 74$ μm; $D_R = 26$ mm; $\omega = 31.4$ s^{-1}; $T \approx 20$°C.

Table II. Effect of the temperature on the breakage kinetic constant, k_1, and the fluid (water) viscosity, η.

T (°C)	k_1 (s^{-1})	η (kg/m/s)
15	1.70×10^{-3}	1.15×10^{-5}
20	0.55×10^{-3}	1.00×10^{-5}

Note: $\langle d \rangle_0 = 400$ μm; $\sigma_d = 74$ μm; $D_R = 26$ mm; and $\omega = 31.4$ s^{-1}.

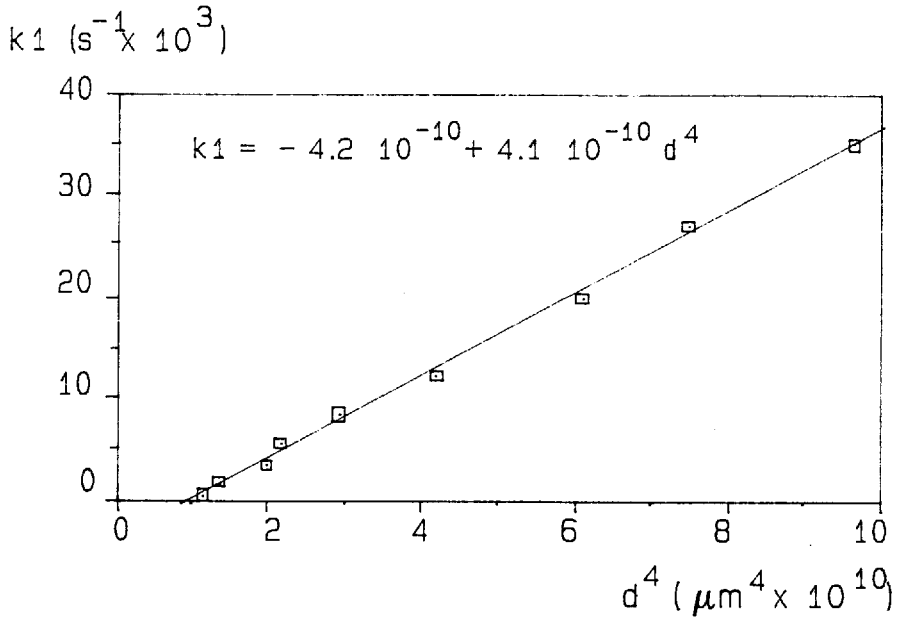

Figure 9. Relation between the mean microcapsule diameter, $\langle d \rangle$, and the breakage kinetic constant, k_1: (D_R = 31 mm; ω = 31.4 s^{-1}; and $T \approx$ 20°C).

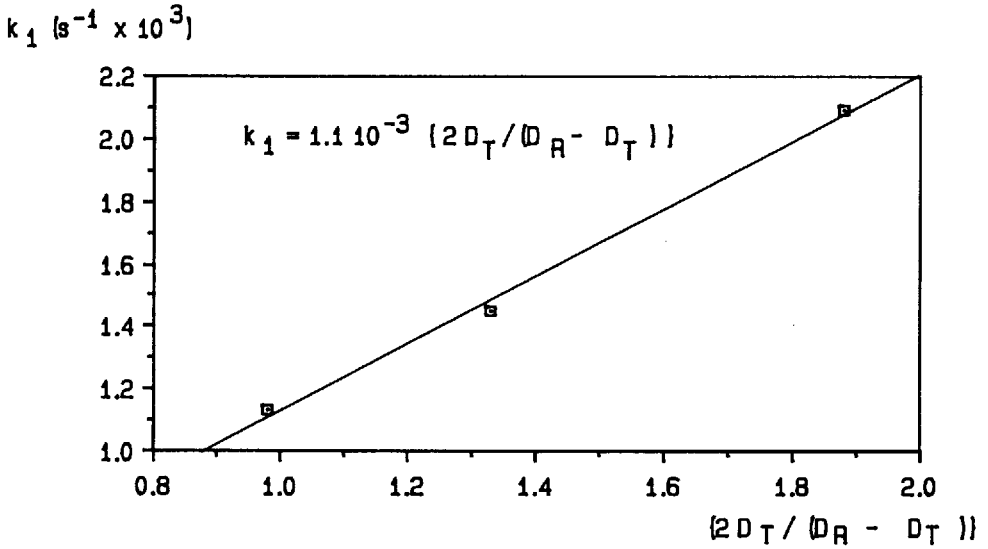

Figure 10. Breakage kinetic constant, k_1 vs. $2D_T/(D_R - D_T)$ ($\langle d \rangle_0$ = 400 μm; σ_d = 75 μm; ω = 31.4 s^{-1}; and $T \approx$ 15°C).

DISCUSSION

Microcapsules as Model System for Breakage Study

Previous work on particle breakage in biotechnology applications related shear to a biological measurement such as biological activity,[13] biomass concentration,[5] or mycelial cell length.[5] From a practical point of view, these studies are very interesting; however, the parameters are not easily correlated with physical effects. For example, the change of bacterial cell activity may be reversible or not, it may be due to a change in membrane transport ability or a true inactivation of the cells. Moreover, it can evolve through mutation or cell selection resulting in increased cell shear resistance. In biological systems, the shear can induce multiple processes, inactivation, change in growth rate or cell, or aggregate morphology. This complexity of the relationship between the shear and its impact on the biological system leads to difficulties in quantifying the shear effects.

Microcapsules constitute a simple (membrane containing one liquid) and symmetrical (sphere) system. Physical properties of the microcapsules, specifically that of the membrane can be determined (membrane elasticity, internal pressure, etc. . . .)[14] and their behavior under different conditions (shear, shock, etc. . . .)[15] can be simulated. The shear can only lead to deformation and breakage pro-

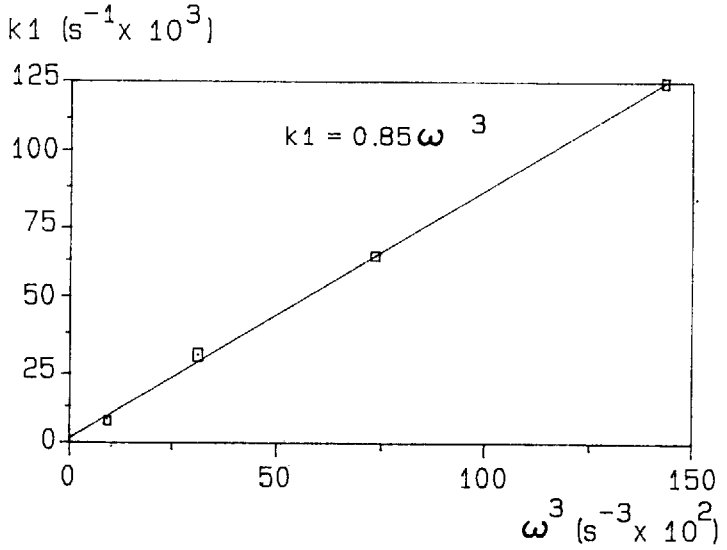

Figure 11. Influence of the turbine angular velocity, ω, on the breakage kinetic constant, k_1 ($\langle d \rangle_0$ = 510 μm; σ_d = 110 μm; D_R = 26 mm; and $T \approx 20$°C).

cesses. Finally, breakage is directly quantified by the concentration of released contents.

Data Acquisition and Microcapsule Size Distribution

The microcapsule sample, prepared by an emulsification process, results in a broad size distribution. Consequently, a size selection of microcapsules is necessary before conducting breakage experiments. This was achieved by sieving the sample under water with gentle mixing to reduce packing and screen obturation. Under these conditions, sieving is slow and inefficient, and some microcapsule damage occurs.

The "soft sieving" is one solution to a broad size distribution. The microcapsule sample characteristics (especially the mean volume, $\langle v \rangle$) remains relatively constant in any size class during the experiment. However, soft sieving presents some significant limitations. The decrease of the mean microcapsule volume, $\langle v \rangle$, during one experiment is as small as the size class range is small or the number of classes is large. In contrast, the precision on the nonbroken numeric fraction, F_n, in a given class increases with the number of microcapsules, $N(c)$, in this given class (smaller number of size classes). The partition of a microcapsule sample into different size classes must be a compromise between these two effects and different class numbers must be tested to find the optimum compromise. The broader the microcapsule size distribution, the more difficult it is to find an acceptable compromise.

The noise associated with the determination of the nonbroken numeric fraction in a given class, $F_n(c)$, can be too high and the experiment must be rejected. Smoothing of raw data was applied to decrease this noise. The kinetic study implicates the determination of parameters that are related with the derivate of the experimental data (breakage rate constant, k). A small deformation of the curve shape may lead to a significant change in the breakage kinetic constant, k_1. For each experiment, a comparison among different smoothing methods must be performed to damp the noise without changing the general curve shape. This involves interpolation from polynomial regression for first and second degree on 3, 5, or 7 points in linear or logarithmic scale for the dependent parameter. The size distribution in the microcapsule samples remains the greatest limitation of the proposed system for the shear study.

Breakage Kinetic Parameters

Viscosity, η, can be a function of the microcapsule volumetric concentration, but for low concentrations such as that used in this study [less than 10% (v/v)], this effect may be ignored. Under these conditions, the breakage process is related to the numeric concentration of microcapsules instead of their volumetric concentration. The true initial concentration of microcapsules is difficult to define. For these reasons, the numeric fraction of nonbroken microcapsules, F_n, was used as the parameter to describe breakage in this phenomenological study.

The activity of a microencapsulated enzyme reactor is generally a function of the volumetric microcapsule concentration (no diffusional limitation) or of the microcapsule surface per unit volume (diffusional limitation). The nonbroken volumetric or surface fraction of microcapsules may be the determinant parameter rather than the numeric fraction. The same observation can be made for several other applications of microcapsules or particles in biotechnology such as sustained release of drugs contained in particles or biological aggregate activity.

The nonbroken volumetric fraction, F_v, is always equal or less than the nonbroken numeric fraction, F_n, and the difference increasing with a larger reduction in mean micro-

capsule volume, $\langle v \rangle$ (Fig. 6). The loss of encapsulated enzyme activity (related to the loss of microcapsule volume) is more important in systems with a broad size distribution. More generally, the sensitivity of one process on the breakage is more important as the process rate is a function of the microcapsule number, diameter, surface, or volume. This effect increases with the dispersion of particle size. In other words, a good control of the particle breakage and dependent processes begins by careful control of the particle size distribution.

Breakage Kinetic Analysis

The observations on the breakage kinetics can be summarized by eqs. (12) and (13), assuming that the shear expression contains the turbine angular velocity, ω, as in eq. (11):

$$F_n = \exp(-k_1 t) \tag{12}$$

and

$$k_1 = f(T) f(d) \langle \gamma \rangle \omega^2 \tag{13}$$

The temperature may have an influence on the hydrodynamics and on the impact of the shear. For example, shear stress, τ, may be the shear determinant parameter for shear effects rather than shear rate, γ. These two parameters are related through the viscosity, η, and the viscosity, η, is temperature, T, dependent. The fluid viscosity, η, may also influence the particle velocity (see below for influence of particle velocity on breakage). A change in nylon membrane rigidity or in the degree of membrane hydration may also explain the temperature influence on the breakage kinetic constant, k_1. A glass transition for nylons in water is reported in the temperature range -15–40°C. Measurements of membrane properties as a function of temperature and breakage rate in different fluids will provide more information on the importance of each effect.

The internal pressure in a spherical microcapsule is given by:[14]

$$P = 4\alpha/d \tag{14}$$

where α is the membrane tension. The disruption of one microcapsule requires the application of an external pressure at least equivalent to its internal pressure. A minimum shear stress, with the same magnitude as this pressure, will result in the breakage of the microcapsule. In a system with a given shear stress, particles smaller than a given size cannot be broken, which agrees with observation (Fig. 9).

The zone of breakage in the turbine reactor is limited to the zone where the shear is equal to or greater than the minimum shear stress needed to break the microcapsule. The volume of this zone may be the shear determinant parameter for the breakage rather than the average or maximum shear stress.

The breakage kinetic constant, k_1, seems strongly dependent on the microcapsule size, d (Fig. 9). Assuming that this constant, k_1, is related to the microcapsule internal pressure, eq. (14) shows a direct dependence of this constant, k_1, to the microcapsule diameter, d. In addition, the membrane tension, α, may be dependent on the microcapsule diameter, d. The membrane thickness may be a function of the microcapsule size, d. Microcapsules are built by coating an emulsified droplet. Internal pressure in the droplet, which follows a similar law to eq. (14) (membrane tension is replaced by liquid surface tension) can have an influence on the membrane structure resulting in varying mechanical resistance with size. Finally, if the breakage occurs at vulnerable points on the membrane, the probability of breakage, and the breakage kinetic constant, can be assumed, in first approximation, proportional to the membrane surface area or to the square of the diameter. These effects can be cumulative and lead to a complex relation.

It is generally assumed that the breakage rate is due to a shear effect. In fact, it may also be due to other processes. The first-order reaction with regard to the microcapsule concentration limits the process to the shear effect or to the shock of one particle with some component in the reactor such as the turbine. Impacts between particles lead to a second-order reaction and may be rejected. Linearity between the breakage kinetic constant, k_1, and the shear rate, γ (Fig. 10), indicates that the shear effect may be the primary process in the microcapsule breakage.

Equation (11) computes an average shear rate assuming that it is constant between the turbine and the reactor wall. Obviously, this is a significant simplification. In addition, the hydrodynamic regime in the reactor is in transition between laminar and turbulent and eq. (11) doesn't take into consideration turbulent effects. In scale up, other relationships[16] may be used to define the average shear rate. Additional experiments must be performed to define where and how microcapsules are broken before proposing a relation between one shear parameter and breakage kinetics.

The angular velocity, ω, appears in the shear rate (γ) expression proposed in eq. (11). This shear rate parameter is only an approximation assuming that the turbine can be replaced by a cylinder. Likely, the shear effects become more important as the particle passes near the turbine blades. Microscopic observation of microcapsules during the experiment shows different possible stages in the breakage process (deformation, cracks in membrane, perforation, membrane wrinkling). The microcapsules may pass several times in the shear zone before breakage. The turbine and the particle movements must be taken into consideration. The velocity of the turbine blade is directly given by the turbine angular velocity. In a turbine reactor, the particle movement in the reactor is a loop with a circulation time inversely proportional to the turbine angular speed.[17] The particle velocity is then proportional to the turbine angular velocity. This logic leads to a relation containing a third power of the turbine angular velocity:

$$k_1 = f(\text{shear rate, blade velocity, particle velocity}) \tag{15}$$

which can explain the relationship between the breakage kinetic constant, k_1, and the third power of the angular speed, ω. In the design of a reactor, turbine angular speed, ω, appears the most important parameter to reduce the particle breakage.

CONCLUSIONS

Microcapsules are a useful model when examining shear effects in biotechnological systems. Both real quantitative and better phenomenological studies of shear can be achieved. They may be used as calibration materials for studies both of shear characterization in a given system and of shear resistance of a particular material. A smaller dispersion of the microcapsule size and a preliminary determination of membrane properties will be a major improvement to these studies.

Control of size distribution and use of very small particles will be a first step in control of breakage. For biological cells, it is not possible to control membrane properties but, in artificial cells such as microcapsules, the choice of an adequate membrane material and of a procedure which gives a membrane with uniform thickness and mechanical properties may limit the breakage. Finally, the design of the reactor system must ensure a homogeneous shear, reducing and providing a uniform number of particles passing through the shearing zone.

NOMENCLATURE

D	diameter (mm)
d	diameter of any microcapsule (μm)
$\langle d \rangle$	mean microcapsule diameter (μm)
F_n	numeric fraction of the nonbroken microcapsules in the total sample or in a given size class (dimensionless)
F_v	volumetric fraction of the nonbroken microcapsules in the total sample (dimensionless)
k	breakage kinetic constant (s^{-1})
N	numeric concentration of nonbroken microcapsules (L^{-1})
n_i	number of microcapsules with a diameter d_i (dimensionless)
P	internal pressure of microcapsules (N/m^2)
r	linear correlation coefficient (dimensionless)
T	temperature (°C)
t	time (s)
V	total volume of nonbroken microcapsules (mm^3)
$\langle v \rangle$	mean microcapsule volume (μm^3)
α	membrane tension (kg/s^2)
φ	microcapsule fraction in a given size class (dimensionless)
γ	shear rate (s^{-1})
τ	shear stress ($kg/m/s^2$)
ω	angular turbine velocity (s^{-1})
η	fluid viscosity (kg/m/s)
σ_d	standard deviation of the microcapsule diameter (μm)

Subscripts

c	refers to a given size class
1	refers to individual microcapsules
0, ∞, or t	refers to time zero, infinity (when all microcapsules are broken) or t
0, 1, or 2	refers to a reaction order equal to 1, 2, or 3
R or T	refers to the reactor or the turbine

References

1. S. E. Charm and B. L. Wong, *Enzyme Microb. Technol.*, **3,** 111 (1981).
2. C. R. Thomas and P. Dunnill, *Biotechnol. Bioeng.*, **21,** 2279 (1979).
3. M. Tirrell and S. Middleman, *AIChE Symp. Ser.*, **74,** (182), 102 (1978).
4. M. Midler and R. K. Finn, *Biotechnol. Bioeng.*, **8,** 71 (1966).
5. R. Bronnenmeier and H. Märkl, *Biotechnol. Bioeng.*, **24,** 553 (1982).
6. N. A. Stathopoulos and J. D. Hellums, *Biotechnol. Bioeng.*, **27,** 1021 (1985).
7. D. Poncelet, M. Constant, F. De Paoli, E.-J. Nyns, and H. Naveau, in *Use of fixed biomass for water and wastewater treatment* (CEBEDOC, Liege, Belgium, 1984), pp. 253–274.
8. A. Ortmanis, R. J. Neufeld, and T. M. S. Chang, *Enzyme Microb. Technol.*, **6,** 135.
9. T. M. S. Chang, *Artificial cells* (Thomas, Springfield, IL, 1972), pp. 20–22.
10. J. H. Rushton, E. W. Costich, and H. J. Everett, *Chem. Eng. Prog.*, **46**(8), 395; **46**(9), 467 (1950).
11. M. Dubois, G. Hamilton, and R. Smith, *Anal. Chem.*, **28,** 350 (1956).
12. R. Bronnemier and H. Märkl, *Biotechnol. Bioeng.*, **24,** 553 (1982).
13. E. Ujcova, Z. Fenel, M. Musflkonova, and L. Seichert, *Biotechnol. Bioeng.*, **22,** 237 (1980).
14. A. W. L. Jay and M. A. Edwards, *Can. J. Physiol. Parmacol,* **46,** 731 (1968).
15. L. Y. Cheng, *J. Biomechan. Eng.*, **109,** 10 (1987).
16. K. Wichterle, M. Kadlec, L. Zak, and P. Mitschka, *Chem. Eng. Commun.*, **26,** 25 (1984).
17. D. B. Holmes, R. M. Voncken, and J. A. Dekker, *Chem. Eng. Sci.*, **19,** 201 (1964).